Two main temperature periodicities related to planetary and solar activity oscillations

Antero Ollila, M Timonen

▶ **To cite this version:**

Antero Ollila, M Timonen. Two main temperature periodicities related to planetary and solar activity oscillations. Aalto University, Emer. 2023, pp.35. hal-04160543

HAL Id: hal-04160543
https://hal.science/hal-04160543

Submitted on 12 Jul 2023

HAL is a multi-disciplinary open access archive for the deposit and dissemination of scientific research documents, whether they are published or not. The documents may come from teaching and research institutions in France or abroad, or from public or private research centers.

L'archive ouverte pluridisciplinaire **HAL**, est destinée au dépôt et à la diffusion de documents scientifiques de niveau recherche, publiés ou non, émanant des établissements d'enseignement et de recherche français ou étrangers, des laboratoires publics ou privés.

Distributed under a Creative Commons Attribution - NonCommercial 4.0 International License

Foreword

This research study article "Two main temperature periodicities related to planetary and solar activity oscillations" has been originally published in the International Journal of Climatology (IJOC) in October 2022. On the 1st of February 2023, the Editorial Office of the IJOC emailed that some claims of scientific errors and unreliable data of this paper have been raised, Appendix 1. We were asked to respond to these claims to be published as a post-publication 'corrigendum' in the journal. Our responses to each claim were emailed back 11th of February, see Appendix. 3rd of April the IJOC emailed that they have decided to retract the paper based on the "s*cientific errors and unreliable data"* in the article. We expressed our objection that the IJOC is not willing to pinpoint what are the claims which we could not clarify or correct in our replies but we did not receive any response. The IJOC retracted the paper 8th of June 2023. We think that the IJOC did not treat our responses according to the normal corrigendum process by detailing the claims, which we were not able to clarify. A very general statement the "s*cientific errors and unreliable data"* is not detailed enough. We emphasized in our responses that none of the original claims questioned the results of our paper. The only data applied in the final analysis is the Finnish Lapland tree-ring index FTPC (2020) applied in tens of reviewed scientific articles. The only data applied in the analysis of the proposed mechanism for 60-year oscillations refers to space dust research results which vary in great quantities; In this sense the evidence includes uncertainties. It should be noticed that so far there has been no generally accepted theory of 60-88-year oscillations. The article below is otherwise the same as the IJOC article but the additions and corrections (two minor editorial errors) have been added in *italic* font. Since the IJOC decided to retract the paper, the agreement between the IJOC and the authors was terminated by their actions.

***

Two main temperature periodicities related to planetary and solar activity oscillations

A. Ollila[1], M. Timonen[2]

[1] School of Engineering, Aalto University, Espoo, Finland, Emeritus

[2] Natural Resources Institute Finland (Luke), Senior Researcher, retired

Corresponding author: Antero Ollila, aveollila@yahoo.com

The second author: Mauri Timonen, matimon@saunalahti.fi

Key Points: 60-year temperature oscillations; 88-year temperature oscillations; AMO; PMO; tree-ring proxies; astronomical harmonic resonances; solar activity oscillations

Abstract

The mechanism and even the existence of the Atlantic Multidecadal Oscillation (AMO) have remained under debate among climate researchers, and the same applies to general temperature oscillations of a 60-90-year period. The objective of this study is to show that these temperature oscillations are real and not artifacts and that these oscillations have different external cosmic origins. The authors have studied how well the variations of astronomical harmonic resonances (AHR) could explain the 60-year temperature variations,

which are based on instrumental records and the tree-ring data of the supra-long Scots pine tree-ring record for northern Finnish Lapland (subsequently called the Finnish timberline pine chronology (FTPC)), stretching to the year 5634 BC. Powerful volcanic eruptions have significant temperature-decreasing impacts, and they are the major disturbances to eliminate in analysis. The similarities between the temperatures of the tree-ring trend and the AHR trend are easy to observe even by the naked eye. The statistical analysis shows that these two signals are statistically related. The analyses also show that the well-known Gleissberg cycle of 80-90 years is the dominating cycle caused by the Suns' activity changes but the observed 60-year cycle can be connected to the AHR cyclicity.

1 Introduction

The first observational evidence for 50- to 80-year temperature oscillations in the North Atlantic basin was identified during the 1980s (Folland et al., 1984; Folland et al., 1986). This phenomenon was later termed the Atlantic Multidecadal Oscillation (AMO) by Kerr (2000). The AMO indices have been based on the average sea surface temperature (SST) anomalies (Enfield et al., 2001) for the North Atlantic north of the equator to 60°N to avoid problems with sea ice changes (Rayner et al., 2003). In the AMO index calculation, the long-term warming signal is normally removed by detrending the SST data and using smoothing of a 10–11 year running mean or similar low-pass filter (Trenberth and Shea, 2006).

The temperature changes are identified in most European countries and in North America as warmer or cooler winter and summer months connected to the phase of AMO. These impacts are not within the scope of this study, but a comprehensive summary can be found in the study of Lüdecke et al. (2020. The IPCC has never included the AMO effects in its GCM (general climate model) temperature simulations *per CMIP5. The control runs covering the last millennium could reveal only ENSO-type periodicities (Mann et al., 2014).* Figure 7.7 of AR6 (IPCC, 2021) is a summary of forcing agents from 1750 to 2019, which shows that the total effective radiative forcing has been 2.70 Wm^{-2}, the sum of anthropogenic agents of 2.72 Wm^{-2} and solar forcing of -0.02 Wm^{-2}. This summary does not recognize any cycling temperature impacts like AMO, which has a positive phase with a magnitude of about +0.3 °C from 2000 to 2020. Researchers have accepted the existence of long-term interannual oscillatory behavior of the global climate system, which is not necessarily restricted only to AMO (Figure 1).

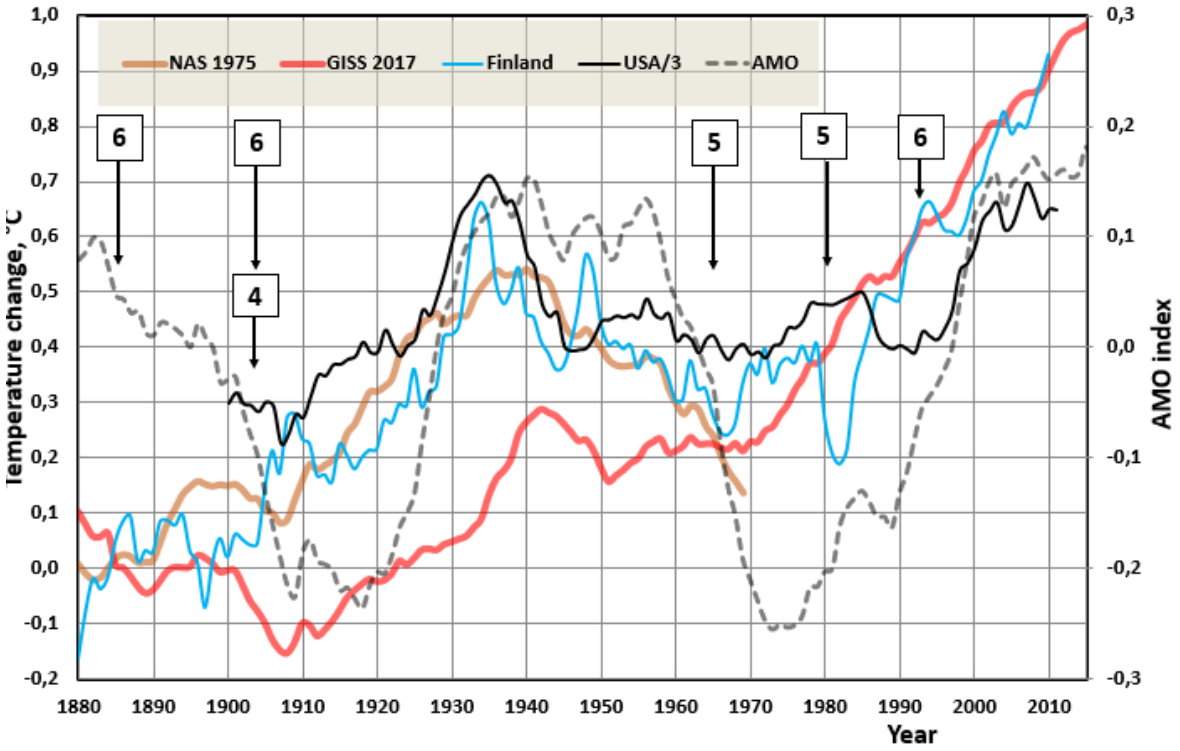

Figure 1. Temperature trends and AMO index (NOAA, 2022b) from 1880 to 2015. GISS (2020) is a global temperature trend of NOAA, NAS (1975) is the global temperature trend used in the report of the National Academy of Sciences, and Finland's temperature anomaly is from (Mikkonen et al. 2014). The temperature anomalies of the USA (NOAA, 2022a) have been divided by three. The numbered boxes with an arrow are major volcano eruptions in the order of the eruption year from left to right: Krakatoa 1883, Mt. Pelee 1902, Santa Maria 1902, Agung 1963, Mt. Ruiz 1985, Mt. Pinatubo 1991. The box numbers indicate the volcanic explosivity index (VEI) on a scale from 0 to 8.

It is easy to see that the temperatures of the USA (NOAA, 2022) and Finland (Mikkonen et al., 2014) follow the oscillatory behavior of AMO. A similar pattern can be noticed in the NAS global temperature trend constructed in the 1970s but very weakly in the latest GISS temperature versions. The temperature amplitude changes in Figure 1 are not directly comparable because there are two regional temperatures and two global temperature trends, but they show that they have a common feature: a cyclic temperature variation during the 1900s. When the AMO changes from a positive to a negative phase, as in the 1940s, the cooling effect of the AMO becomes dominant over the greenhouse gas effects and causes the global temperature to decrease, which happened from 1940 to 1975. Similarly, when the AMO turns from a negative to a positive phase, global warming accelerates, as it did after 1975. A similar oscillation mode of about 60 years with an identical time scale has been identified in the northern part of the Pacific and has been termed the Pacific multidecadal oscillation (PMO) by Chen et al. (2018).

As Figure 1 indicates, the AMO and PMO are probably connected to global-scale multidecadal oscillation (GSMO), also called Global-Scale Multidecadal Variability of about 50 to 70 years. Klyashtorin et al. (2009) have shown that climatic indices of the Arctic region have undergone 50–70-year fluctuations during the last 1500 years. About the same oscillation period of 65–70 years was found by Schlesinger and Ramankutty (1994) in analyzing global and regional temperature trends from 1850 onward, and they concluded that the oscillation was the result of 50–88-year oscillation of the North Atlantic Ocean. Roberts et al. (2007) utilized empirical mode decomposition for day length and magnetic field variations, and they found periodicities of 62±3 years and 58±5 years. Rohde et al. (2013) analyzed the observed based global temperature trend from 1753 to 2011. They found that GSMO is related to AMO, but there are also differences that could be explained by different dynamical delays of oceans and land.

The researchers of astrophysics have been interested in the cyclic behavior of solar magnetic activity since 1843 when it was discovered by Schwabe (1843) to have about an 11-year duration. Hale (1908) discovered the magnetic nature of sunspots and that the complete magnetic cycle spans two solar cycles (22 years). Gleissberg (1958) found that the solar cycles weaken and strengthen in the period of about 80-year by applying a lowpass filter to the sunspot number records. Siscoe (1980) found an 80-year periodicity in the auroral records, and Feynman and Fougere (1984) identified a strong periodicity of 88.4±0.7 years in the 1000 years long auroral records.

A new opportunity was opened to researchers when the records of cosmogenic isotopes like ^{14}C and ^{10}Be became available covering the whole Holocene. The sediment study of Agnihotri et al. (2002) demonstrates 60±10-year periodicities during the last 1200 years matching well with Indian monsoon intensities. The sediment study of Patterson et al. (2004) along the NE Pacific coast studying ^{14}C and ^{10}Be cosmogenic nuclides, from an interval 1440-4495 years before the present time, identified cyclicity of 50–85 years. Lin et al. (1975) identified an 80-year periodicity of broad maximum in the ^{14}C data of tree-rings. Attolini et al. (1987) found an 88-year periodicity in the cosmogenic isotopes. Cini Castagnoli et al. (1992) found a 55-60 years period in sea carbonates with unknown source and 87-90 years periods ^{14}C in tree-rings. Ogurtsov et al. (2002) applied modern statistical methods for analyzing sunspot numbers and cosmogenic isotopes during the last millennium, and the results showed a 50–80-year periodicity. Peristykh and Damon (2003) identified the dominating periodicity of 87.8 years with 84.6±0.1 and 91.5±0.1 sidebands in the spectral analysis of cosmogenic ^{14}C data originating from the tree-ring data with one-year accuracy over 12,000 years. The period of about 60 could also be identified.

These research results with many others confirm that the Gleissberg cycle of about 88-year periodicity is a real phenomenon showing that the Sun's activity varies over long time periods and is, therefore, an essential agent in modern global warming. The periodicity of the 88-year Gleissberg cycle like the 220-year Suess (1980) cycle and the 2200-2400 Hallstatt cycle can be linked to the 22-year Hale cycle and the 11-year Schwabe cycle.

The periodicity of about 60-years has been identified in the research analyses, which differs from the Gleissberg cycle. This shorter periodicity matches the AMO/PMO cycle and its origin is the main interest of this study. There is no commonly accepted reason or mechanism for AMO, PMO, and GSMO, and the debate is ongoing among researchers. There are four major categories for the suggested AMO mechanism.

The most common explanation of AMO is internal oscillatory behavior related to Atlantic meridional overturning circulation (AMOC) (Trenberth and Shea, 2006; Ting et al., 2009; Knight, 2009; Wu et al., 2011; DelSole et al., 2011; Zanchettin et al., 2014; Zhang, 2017). AMOC is characterized by a northward flow of warm and salty waters in the upper layers of the Atlantic like the Gulf Stream, and a southward flow of cold and deep waters, which are part of the global thermohaline circulation. This explanation has been regarded by some researchers as an explanation for global warming that is an alternative to anthropogenic reasons.

This explanation can be criticized on two bases. First, any oscillation needs energy. If there were no oscillating external energy flow like solar irradiance into the thermohaline system, it would stop; if solar irradiation is about constant, there would be no oscillations, and this is the assumption of the IPCC (2021) that the Sun's activity has been practically constant since 1750. The second reason is the unknown time scales of thermohaline systems, which vary from centuries to a millennium. On the other hand, the Gulf Stream flows from Key West to the Arctic Ocean in about three months, and the cold currents' flow southward cannot be much longer. The time scale of about one year matches the 11-month delay of CO_2 concentration response to the Southern Ocean temperature change (Humlum et al., 2013), but none of these time scales match the 60-year period of AMO.

The second group of studies (Clement et al., 2015; Clement et al, 2016; Cane et al., 2017) have concluded that AMO is the result of stochastic atmospheric forcings. This explanation can be criticized in that stochastic changes should not be able to cause oscillation with about a 60-year period.

The third group of studies (Booth et al., 2012; Bellucci et al., 2017; Murphy et al. 2017; Bellomo et al., 2018; Haustein et al. 2019) show that the external radiative forcings by anthropogenic GH gases and tropospheric aerosols explain the AMO of the twentieth century. This observation is not in line with the almost constant growth rate of GH gases without decreasing periods, and there is no systematic concentration dataset of aerosols.

The fourth group of studies (Mann et al., 2014; Frankcombe et al., 2015) has concluded that AMO probably exists, but it is difficult to separate external forcings from internal variability. Mann et al. (2021) have concluded in a recent study that there is no compelling evidence for internally driven AMO, but they found statistical evidence using CMIP5 (the Fifth Phase of the Coupled Model Intercomparison Project) simulations that apparently AMO-like oscillations were driven by pulses of volcanic activity during the last

millennium. This conclusion can be criticized in that CMIP5-like models cannot reliably simulate climate internal variability or the surprising pause of the 2000s, which has been the subject of more than 200 scientific research publications without a common understanding in the climate community. It is well-known that strong volcanic eruptions can cause global temperature decreases from 0.3 to 1.0 °C for 3–10 years. Figure 1 shows three eruptions after 1881 with the VEI of 6, and the temperature effects can be identified but they are not always significant. Volcanic activities cannot explain the increasing trends of temperature oscillations.

The purpose of this study is to analyze temperature oscillations during the last millennium utilizing paleoclimatology data and instrumental records and to test whether approximately 60-year GSMO temperature oscillation can be found in global temperature trends and in AMO and if it is connected to external forcing originating from solar system oscillations. Since the 60-year and 88-year oscillations happen simultaneously, the combined effects have been compared to the tree-ring data.

2 Methods and Material

2.1 Material and Data

The following global temperature data sets have been applied: NAS (1975), GISS (2020) data of NOAA, and HadCRUT4 of the Met Office Hadley Centre (2020). Local temperature data sets have been used for the USA (GISS, 2022a) and Finland (Mikkonen et al., 2014).

The tree-ring index data sets of Briffa, Mann, Crowley and Lowery, Overpeck, and Jones's temperature data set are from the data repository NCDC (2020). The calibration procedure of this data has been explained in the article of Briffa et al. (2001). Ljungqvist paleotemperature data set is from his study (Ljungqvist, 2010). The Finnish Lapland tree-ring index FTPC (2020) is the basic tree-ring data set applied for analyses.

The Sun activity estimate is from Lean (2010), and the Sun speed calculations have been carried out by Ollila (2017) applying the Horizon application of NASA (2017).

The AMO index is from NOAA (2020b) and the PMO index is from Chen et al. (2016).

2.2 Methods

Fast Fourier transform (FFT) has been used to calculate the amplitude spectrum of the temperature proxy series and the AHR signal, applying the existing function of Excel. The FTPC data were from 1005 to 1993, the Ljunqvist data from 5 to 1975, and the AHR data from 1005 to 2028. The AMO and PMO signals, which are based on the detrended sea surface temperature trends, are readily available. Since a global 60-year oscillation periodicity has been detected, the detrended global temperature signal has been calculated in relation to the nonlinear temperature trendline of HadCRUT5.1 from 1856 to 2015 applying a second-order *polynomial* equation $T = 517.29 - 0.2587 * yr + 0.00006805 * yr^2$.

3 Analyses and results

3.1 Astronomical harmonic resonances - AHR

Ermakov et al. (2009) were the first to introduce the theory that planetary orbits have an influence mechanism on temperature variations through the variations in space dust entering the Earth's atmosphere.

Scafetta (2010) has analyzed in detail how the orbital periods of Jupiter (11.86 years) and Saturn (29.42 years) create conjunction periods of about 20 and 60 years, causing temperature variations with peak-to-peak amplitude of about 0.1 °C and 0.25 °C, respectively. Because there is so much evidence about the 60-year oscillation in the climate system of the Earth, the astronomical harmonic resonances (AHR) phenomenon is a potential explanation.

Ollila (2017) has combined these two theories by introducing new details to the AHR. Gold (1975) has pointed out that the small particles in the solar system spiral toward the Sun, but they may become trapped in resonances with the planets. This should result in a circumsolar dust cloud, which is not uniform. Dermott et al. (1994) have shown by numerical simulations that the dust particles are trapped in a 5:6 resonance with the Earth. The optical measurement of the infrared astronomical satellite (IRAS) revealed in 1983 that the Earth is really embedded in a circumsolar toroid ring of dust (Wyatt et al., 1999), which co-rotates around the Sun with Earth, and this ring locates from 0.8 AU to 1.3 AU from the Sun. In the wake of the Earth is a permanent trail of dust particles, having about 10% greater density than the background zodiacal cloud (Dermott et al., 1994).

Cosmic dust, also termed interplanetary dust, micrometeoroids, or micrometeorites, has a size distribution from 0.001 to 100 micrometers (Ermakov et al., 2009). The dust is composed of sulfides, silicon carbides, amorphous silicates, carbon monoxide, ice, polycyclic aromatic hydrocarbons, and polyformaldehyde. Particle density is from 1 to 3 g/cm3 (Krihna & Durbha, 2013), and the quantity of dust particles is 100–1000 per cm3 (Ogurtsov & Raspopov, 2011). The main origin of cosmic dust is Jupiter family comets (80–85%), and the rest is from asteroids, Halley-type comets, and Oort cloud comets (Carillo-Santchez et al., 2017; Nesvorny et al., 2010).

Lidar radar, in situ dust instruments onboard the Ulysses and Galileo spacecraft, micro craters on spacecraft, accumulation on polar ice cores, and deep-sea sediment observation methods of the dust amount entering the Earth's atmosphere have been applied. Estimates of the amount of cosmic dust entering the Earth's atmosphere vary from 41 tons daily (Rojas et al., 2021) to 10,000 tons (Ermakov et al., 2009). A middle-range daily estimate is from 110 tons (Gardner et al., 2014) to 300 tons (Plane, 2012).

The dust particles become ionized in the Earth's magnetic field. They have an important role in creating cloud condensation nuclei (CCN) because 40–70% of global CCNs have been estimated to originate from nucleated particles (Dunne et al., 2016).

Variations in dust amounts happen during a longer time scale depending on the periodicities of the planets, which can move the dust cloud's position in the Earth's orbit. The periodicities caused by Jupiter and Saturn can be found in the calculated speed variations of the Sun around the solar system barycenter (SSB). Horizon's application (NASA, 2017) can be used to calculate accurate locations and motions of solar system planets and the Sun. If Jupiter and Saturn are removed from the planetary system, the Sun's movements disappear almost totally, and this finding connects the AHR effect to these giant planets.

Scafetta (2010) has proposed that the cosmic dust variations affect the Earth's magnetic field oscillations, and Ermakov et al. (2009) have proposed that the varying amounts of dust entering the atmosphere change the cloudiness and, further, cause temperature variations. Since the Earth's magnetic field also oscillates (Roberts et al., 2007) with about the same periodicity of 60 years, these two effects may be connected. In his pioneer research, Svensmark (1998) proposed that solar activity variations modulate galactic cosmic ray fluxes, which can also nucleate clouds. In this case, these two mechanisms have a common final step in affecting temperature variations.

As summarized in the Introduction section, there are four major categories for the suggested AMO mechanism but none of them is generally accepted. The AHR mechanism is the fifth category.

3.2 Tree-ring analysis and the FTPC data set

Climatic variations leave their mark on many chronologically recorded natural phenomena, such as annual rings of trees. The discipline of the study of tree rings is called tree-ring science or dendrochronology. The so-called pine subfossils (megafossils) that once sank into the swamps and the bottom mud of lakes remain measurable under cold and oxygen-free conditions for millennia, making it possible to study variations in the Holocene climate retrospectively.

With the development of dendrochronological methods and the global expansion of research data, the time perspective of research has expanded from days and months to thousands of years, which has strengthened the position of the dendrochronology discipline,

especially in the study of environmental change. The annual tree rings are the most effective form of occurrence of proxy information describing the climate.

Information about changes in the properties of the soil and atmosphere is stored in annual tree rings and individual cells. Their thickness growth (tree-ring width) is regulated by the average summer temperature in cool areas and precipitation in arid regions. Thus, depending on the study area, variations in annual tree rings indicate changes in temperatures or precipitation. The knowledge that the minimum factor for pine growth in Lapland (the northern part of Finland) is temperature provides an opportunity to draw up a barcode-like pattern based on tree-ring widths (Figure 2). Especially in Lapland, annual tree rings can be used to estimate the temperatures during the growing season with good results (Helama et al., 2002).

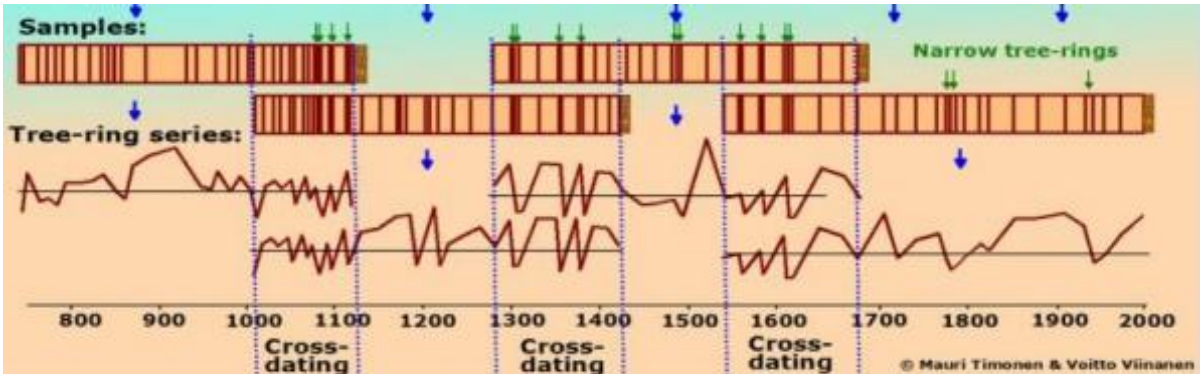

Figure 2. Compiling the tree-ring data by the cross-timing of tree-ring samples.

For timing tasks, a reference series (master) describing the climatic variations of the region is usually available, in which case the correct timing can be found by comparing the sample with it. This requires measuring the tree-ring series with a tree-ring microscope. Scheduling is easiest with scheduling programs that correlate, for example, 50-year segments.

When trees have been grown at different times, the tree rings can be combined if the trees have lived for at least a few decades at the same time, as depicted in Figure 2. By comparing (cross-dating) and statistically testing the segments of the measurement series and master series, the best matches can be found. For special cases such as when the correlations are at the limits of statistical significance (weak climate signal), quality checks of the limit timberline pine in Lapland can be executed with special programs.

As described above, time series of up to thousands of years can be built, provided that a sufficient number of overlapping tree trunks are provided. The dating of annual tree-ring samples is easily carried out on Lapland conifers (pine and spruce); in most cases, it is sufficient when specimens or disks taken from two different trees have a common cover of at least 30 tree rings.

Lapland's forest border pines are particularly useful for climate research due to their strong response to the average July temperature. It is an ideal tree species for studying long-term variations in growth, as its wood material is preserved for thousands of years thanks to resin, tar, and other chemical components. Lapland pine survives as a standing tree or a trunk on the ground without decaying for hundreds of years. In cold, low-oxygen lakes and swamps, trunks buried in mud can remain undecayed for thousands of years.

The annual tree rings are part of a wider group of proxy variables. However, the tree rings are in a special position, as they are the only representative of the year-accurate proxies. The year accuracy has also provided an opportunity for more detailed targeting of variations in the Holocene climate, which is of great importance, for example, in the precise dating of volcanic eruptions.

Perhaps the most significant property in the year accuracy of tree rings is the avoidance of the resolution error that leads to the averaging of the data.

Year accuracy implies better compatibility when combining instrumental and proxy measurements. Of course, the temperature estimates obtained from tree rings are model-based calculations, but the temperature estimates obtained from the modeling are easy to scale to correspond to the variation in the temperature-measurement data. This significantly increases the usefulness of tree-ring data for accurate climate analyses.

The measure of tree-growth variability is the annual tree-ring index. It is calculated by comparing the radius growth with the smoothing curve representing the average growth. A smoothing curve considers the rapid growth rate of a young tree and the elimination of the slower growth rate of an aging tree.

The calculation of the indices is based on standardization, which means making the growth of trees that have lived in different conditions comparable with each other so that they can be combined and averaged into annual tree-ring series. For example, at least 31 observations per calendar year are required in Inari (the northern part of Lapland) if an indexing accuracy of 10% is sought at a 95% confidence level.

An annual tree-ring index is a relative number that receives a value of 100 for each calendar year in the case of an average summer. In the calculation of tree-ring indices, a growth event is considered an entity that is divisible into its components. Cook's conceptual model (1992) provides a good starting point for the division; the growth event is divided into its parts: the biological aging of a tree, weather, and climate factors, factors internal to the stand, external factors, and unexplained factors.

The aim of standardizing research data on climate variation is to eliminate the effect of biological age on growth. However, it is not enough if the data include noise that interferes with the climate signal. It can be removed both by modeling and by limiting the data in

advance. In tree-specific modeling, each tree is standardized separately. It is perfectly applicable for the analysis of annual and decadal variation.

The completion of the FTPC (2021) in 2002 showed that useful tree-ring chronologies can be developed from subfossil pines for the needs of climate research. When the coefficient of variation is known and the desired accuracy of the index estimate and statistical significance is determined, the sample size can be determined.

3.3 Observed cyclic temperature variations

Figure 3 depicts the cyclic variations of AMO, PMO, AHR, and global temperature (Met Office Hadley Centre, 2022).

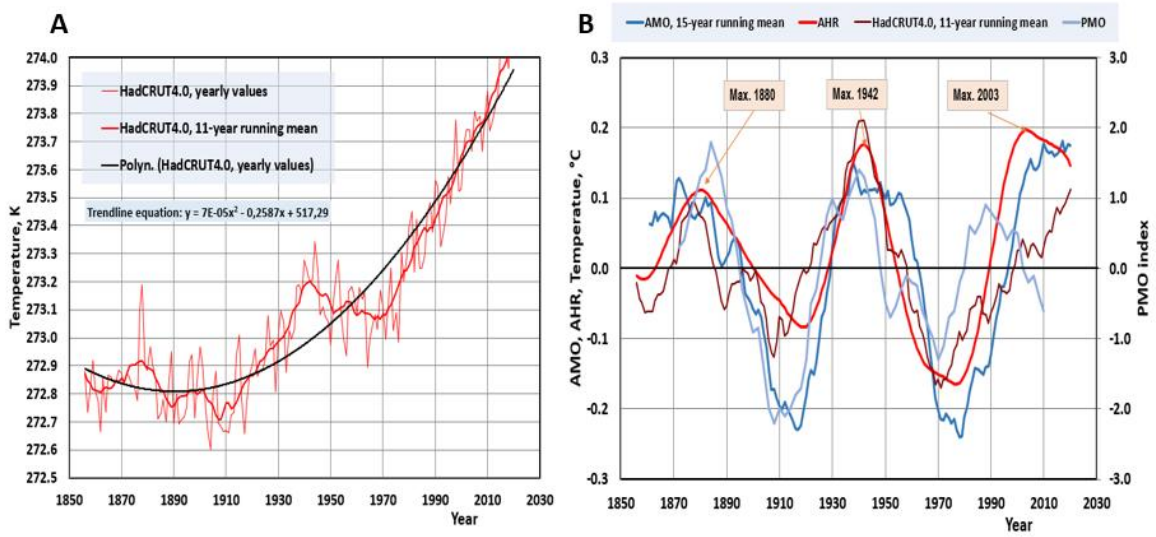

Figure 3. *A. Yearly, 11-year running mean, and trendline selection used for detrending HadCRUT4.0 temperature data. B. The 60-year fluctuations of AMO, PMO, AHR, and temperature trends. The AHR trend is from the study of Ollila (2017), and the PMO has been digitized from Figure 5 of Chen et al. (2016) with 2-year steps.*

The periodicity of the variables defined as cycle lengths is practically the same. AMO and PMO amplitude variations are greater than the global temperature variations, and it is natural since the northern parts are more sensitive to temperature changes. The PMO shows a 50-year oscillation period from 1940 to 1990, but otherwise, it has the same oscillation characteristics as AMO.

The AMO index is not available before 1860, and therefore the analysis can be carried out before 1860 only by using paleotemperature data of proxies. In Figure 4 some most used temperature trends based on tree-ring methods have been depicted, and they are available from the data bank maintained by NOAA which was originally processed by Briffa et al. (2001).

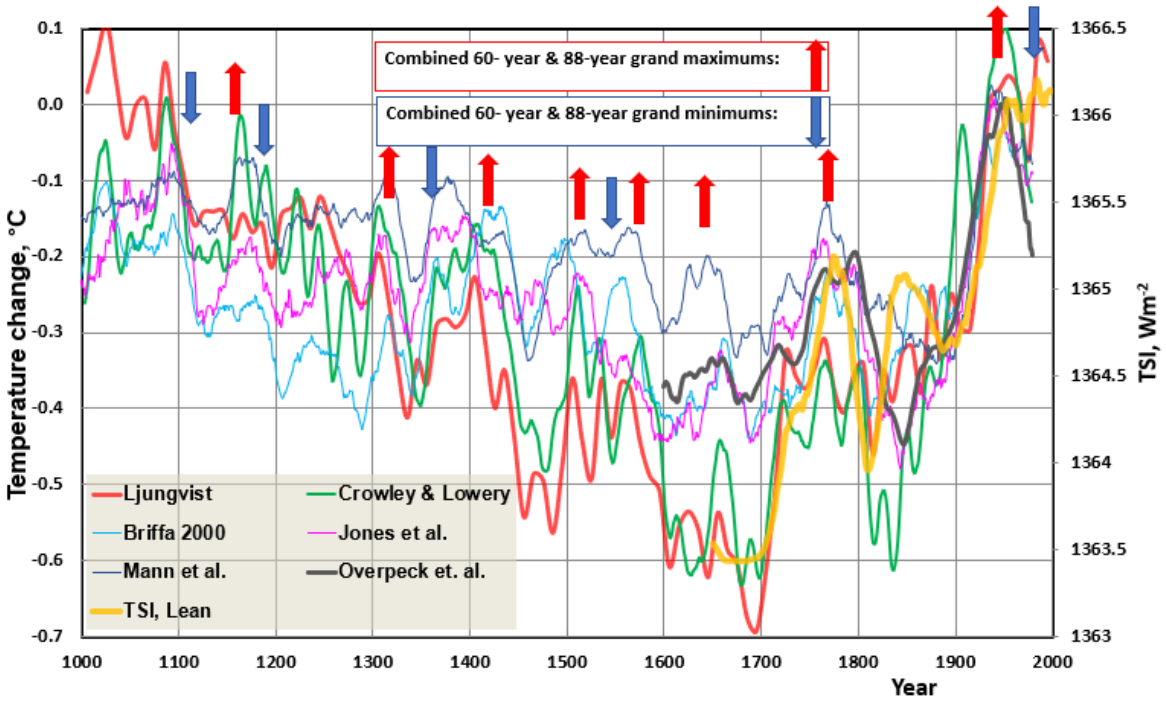

Figure 4. The paleo data of different temperature proxies during the last millennium and the TSI (total solar irradiation) value of Lean et al. (1995). The temperature data of Ljungqvist (2010) include nine types of temperature data, namely two historical documentary records, three marine sediment records, five lake sediment records, three speleothems $\delta^{18}O$ records, two ice-core $\delta^{18}O$ records, four varved thickness sediment records, five tree-ring width records, five tree-ring maximum latewood density records, and one1 $\delta^{13}C$ tree-ring record. Because of the combination of different trends, it is rather heavily averaged and is available only as decadal average values, being unsuitable for intra-decadal analyses.

Lean et al. (1995) have reconstructed the TSI trend from 1610 onward by using revised sunspot activity records and the correlation between sunspot darkening and faculae brightening (bright areas between sunspots). They have compared their TSI reconstruction to tree-ring data and ^{10}Be cosmogenic isotope records and found good consistency.

The purpose of depicting the Ljungqvist temperature trend and Lean's TSI trend in the same figure as tree-ring trends is to show that different kinds of temperature proxies have common features. The 60-year oscillation and an 88-year highlighted points of time will be explained in section 3.4. It is obvious that the 60-year and 88-year oscillations cannot explain the overall cooling from 1000 to 1700 and overall warming from 1700 onward in Figure 3.

Only the Crowley and Lowery tree-ring trend and Ljungqvist trends have the low-temperature values of the Little Ice Age (LIA) during the 1600s. This is supported by the

TSI (total solar irradiance) estimate of Lean et al. (1995), which follows very well the warming trend starting about 1700. Otherwise, the depicted proxy temperature trends have many common features.

3.4 Time domain analyses

The longest 7000-year conifer tree-ring chronology in Eurasia has been extended to 5634 BC (Helama et al., 2002), and these data have been used in further analyses of this study. The oldest parts of the chronology are based on pine megafossils found in the small lakes of Finnish Lapland, which is nowadays a tundra-forest region. This tree-ring chronology is sensitive to temperature changes because the temperature of the summer months is the key factor in tree growth in the cold climate conditions of the region. The 11-year running mean of this data has been depicted in Figure 5. It should be noticed that this data does not include long-term trends since it is detrended.

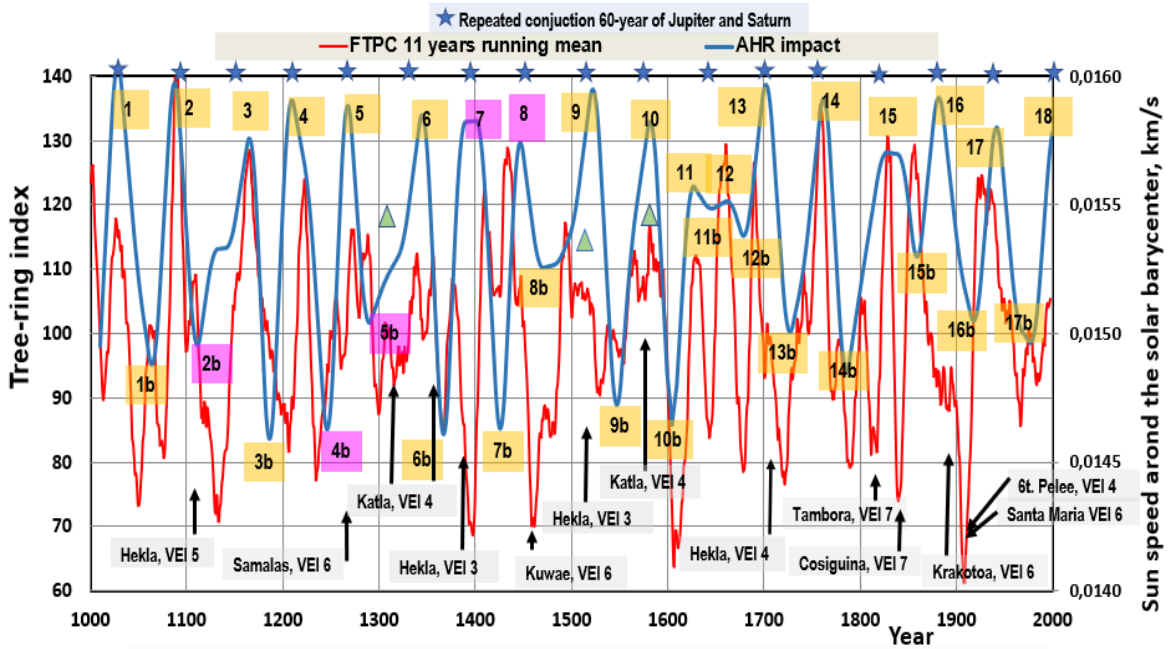

Figure 5. The supra-long Scots pine tree-ring record for northern Finnish Lapland from the year 1000 onward does not include century-scale variations. The Sun speed variations around the solar system barycenter are depicted according to the maximum envelope values of 20-year cycles representing AHR impact. The years of repeated combined orbits of Jupiter and Saturn with 59.6-year periods have been depicted and marked with asterisks. The green triangles close to peaks 6, 9, and 10 are from the detrended data of Crowley & Lowery from different Northern Hemisphere sites, which have higher peak values than FTPC, probably due to the impacts of stronger Hekla and Katla eruptions on the FTPC data.

AHR impact is based on the Sun's speed changes around the barycenter calculated by the Jet Propulsion Laboratory Horizons internet application (NASA, 2020). Eighteen maximum peaks and seventeen minimum peaks have been numbered, and it can be noticed that the

Jupiter–Saturn repeated 60-year conjunctions do not happen simultaneously with the AHR maximum value, but they are close. The oscillation of the AHR signal varies during the last millennium, not always being sinusoidal in shape. The greatest disturbance is during the LIA, when there are two low peaks in the 1600s when there normally would have been one high peak only. Of course, this creates a question of whether this deviation has something to do with the low temperatures of the LIA.

Naked-eye analysis of the similarities between the AHR signal and the tree-ring signal show that generally the peaks happen simultaneously. The peaks 7, 8, 9, and 16 are exceptions when it looks like instead of a maximum peak, there is no maximum peak, or it is even a minimum peak. The reasons can be detected from the information in the lower part of Figure 4, and they are four powerful volcanic eruptions happening during the maximum effect of these AHR peaks in question. The Hekla eruption (VEI 3) in Iceland starting in 1389 resulted in a negative deviation in the tree-ring index. The Kuwae eruption (VEI 6) in Polynesia in 1452–57 stopped the maximum tree-ring index growing and turned it into a minimum peak. The Hekla eruption (VEI 3) in 1510 did the same thing. The Katla (VEI 5) eruption in 1625 and the Katla (VEI 4) of 1660 reduced the peak values during those years. The Krakatoa eruption (VEI 6) in 1883 also turned the tree-index value into the minimum value.

Kuwae's magnitude index in 1452-53 is VEI 6, but Gao et al. (2006) have analyzed the released sulfate dust amounts, and they found that Kuwae's dust amount probably surpasses the same of the Tambora event, making the Kuwae eruption the greatest during the millennium. The Hekla eruption (VEI 4) in 1845–46 caused the maximum peak number 4 firstly to decline, and later the tree-ring index reached the maximum value simultaneously with the AHR signal. The Samalas eruption (VEI 6) 1257 happened simultaneously with the minimum AHR, and it caused the deep minimum tree-ring index value.

The Katla eruption (VEI 5) in 1721 strongly decreased the minimum value of peak 13b, and in the same way, the Laki eruption (VEI 4) in 1785 reduced the minimum value of peak 14b. The Tambora eruption (VEI 7) caused a strong negative tree-ring deviation during the maximum AHR impact, but the tree-ring value increased to a normal maximum peak value after 13 years of Tambora eruption. Seven years later, in 1835, the Cosigüina eruption (VEI 7) in Nicaragua caused another deep decrease in the tree-ring index of 1837 during the AHR maximum. The third strong volcanic eruption during the 1800s was Krakatoa in 1885. Due to these eruptions, the temperature impacts of 60-year and 88-year cycles were much smaller than otherwise expected in the 1800s.

There is a logical explanation as to why the volcanic eruptions in Iceland have a strong influence on the temperatures and tree growth in Finland. The reason is the westerly wind pattern, which is dominant in Finland, and these winds in the troposphere bring a lot of volcanic ash particles to Scandinavia from Iceland *(Kalliokoski et al, 2020).* Therefore, the impacts of lower severity index eruptions like VEI 3 in Iceland may have the same impact as the VEI 6–7 index in other parts of the world. As a curiosity, it can be mentioned that the tree-ring index of Crowley and Lowery (Briffa, 2001) has no negative temperature effect on

the peaks of numbers 7 and 9 as marked in Figure 2 when Hekla eruptions have decreased tree growth in Finland.

Normally the global temperature effects of explosive volcanic eruptions are based on the ash columns reaching the height of the stratosphere. It takes about six months for volcanic aerosols to spread over the globe, and therefore these most powerful eruptions have global temperature-decreasing effects. In the best recorded volcanic eruption of Mt. Pinatubo (VEI 6) in 1991, the temperature effects could be measured globally for five years (Ollila, 2016). Therefore, volcanic eruptions cannot always perfectly explain the observed tree-ring anomalies like that of Hekla in 1100, and Hekla in 1390. The temperature effects last longer than could be expected based on our present knowledge of eruption impacts. The unknown factors of seasonal conditions may have negative impacts on latewood production.

When there are no major volcanic eruptions during the AHR maximum effect, the tree-ring maximum happens simultaneously with a sharp peak like during peaks 1, 2, 3, 4, 10, 14, and 17. It can be concluded that volcanic eruptions do not cause the AMO, PMO, or GSMO effects, but they act like disturbances, especially during the maximum effects of the AHR.

The author used the cycle periods of the AHR cycles and the tree-ring cycles for carrying out a statistical analysis. The cycle periods of peaks 7, 8, and 9 were not used for calculating the cycle times between the peaks due to the inaccurate peak estimation caused by volcanic eruptions. The timing of negative peaks did not have this problem. The tree-ring data were applied to the year 1859, and thereafter the instrumental data were applied as depicted in Figure 2.

The period from 1087 to 2003 encompasses a total of 17 positive peak cycle times and 16 negative peak cycle times, which are collected in Table 1.

Table 1. The cycle lengths of positive (light red) and negative (light blue) peaks of AHR and FTPC signals.

Year	AHR	FTPC	Year	AHR	FTPC
1087	58	60	1111*	47*	83*
1164	77	76	1186	75	73
1209	45	57	1246*	60*	28*
1267	58	51	1290*	44*	65*
1344	77	66	1367	77	67
1400*	56*	70*	1426	59	59
1447*	47*	25*	1470	44	36
1522	75	74	1547	77	93
1581	59	73	1604	57	52
1626	45	48	1645	41	37
1661	35	31	1679	34	35
1702	41	43	1727	48	43
1761	59	55	1785	58	65
1827	66	70	1859	74	73
1881	54	50	1911	52	49
1941	60	63	1977	66	63
2003	62	62			
Average values: AHR 57.2 years, FTPC 57.4 years					

The periods of the AHR signal vary from 35 to 77 years and the tree-ring index from 25 to 76 years, respectively. The linear regression fitting between all AHR and FTPC periods gives the coefficient of determination $r^2 = 0.80$, if five peak values marked by asterisks in Table 1 (2b, 4b, 5 b, 7, and 8) have not been included, and the coefficient of correlation is 0.90. It is a piece of strong scientific evidence that the AHR is the external forcing factor causing the GSMO, PMO, and PMO. These different temperature oscillations have the same external origin. It also explains why these oscillations happen almost simultaneously. It should be also noticed that the variation of the AHR period significantly improves the correlation to FTPC periods in comparison to the constant 60-year period. It is worth noting that two AHR cycles with a length of 35 and 45 years in the 1600s, shorten the average AHR cycle length to 57.2 years, but the notation 60 years has been used because it is the median length.

The observed temperature variation amplitude from 1850 to about 1910 decreases, as Figure 1 indicates. The reason is strong volcano eruptions (Krakatoa, Mt. Pelee, and Santa Maria), as Figure 4 shows. This may raise doubts about whether the planetary influence is a consistent phenomenon. The long-term tree-ring analysis has an advantage over

temperature data in showing that the 60-year oscillation during the preceding centuries has been as strong as during the last 100 years.

3.5 FFT analyses

The cycle length analysis of section 3.3 may be prone to subjective interpretation and therefore another signal analysis method was used. The spectral analysis applying the fast Fourier transform (FFT) was carried out for the AHR from 1005 to 1975, FTPC from 970 to 1993, and Lungqvist proxy temperature signal from 5 to 1975. The results are depicted in Figure 6.

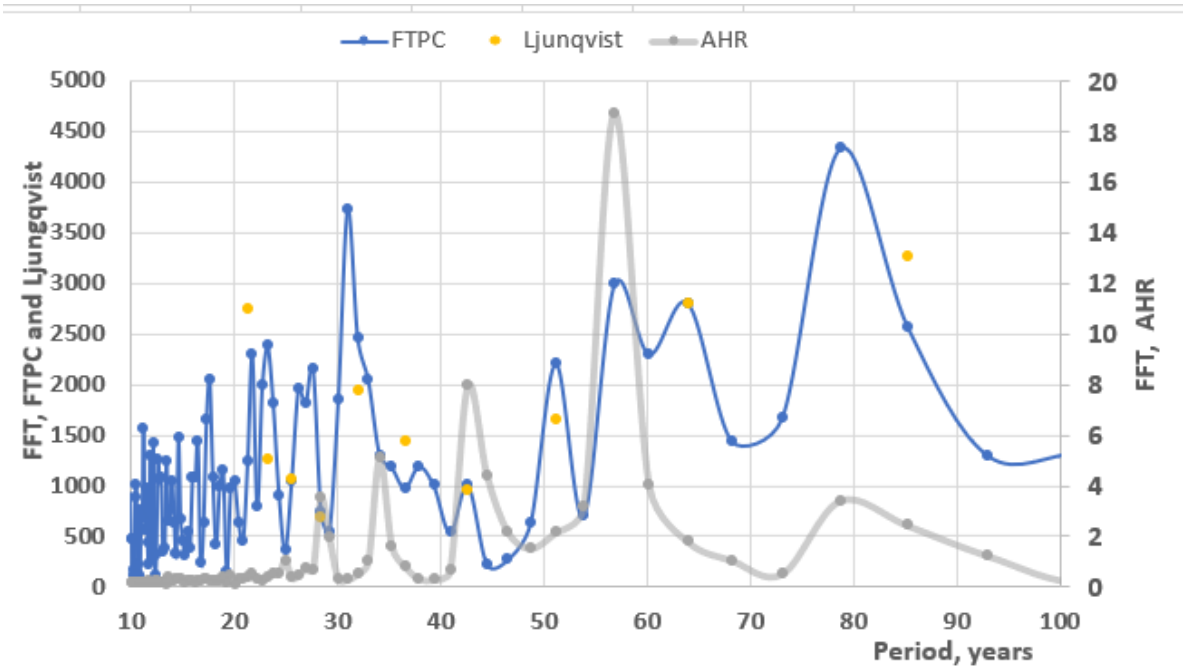

Figure 6. The FFT values of AHR, FTPC, and Ljungqvist signals.

The results show that the AHR signal has a very clear dominant period of 57 years as expected (Table 1), and there are three other periods of 43, 34, and 79 years. The FTPC signal has the greatest value for 79 years but the maximum peak of it is broad indicating that there are other periods close to the peak value of 79 years. The other significant periods are 34 years and a double peak for the periods from 57 to 64 years. The Ljungqvist signal has a 10-year sampling period and it is the combination of several different types of proxy signals. The FFT values show that the dominant period is around 85 years, and the second most significant peak is of 64 years.

Considering the earlier research studies referred to in section 1 and the results of this study, the Gleissberg periodicity is about 88 years with uncertainty limits of +2 years –10 years, and the AHR periodicity is about 60 years with uncertainty limits of +4 years –4 years. Smaller uncertainties have been reported in individual studies, but considering all the studies, large uncertainties are justified.

There are potential physical explanations for the spread of periodicities. The Schwabe cycle length varies from 10 years to 14 years, and it may cause the spread to the Gleissberg period because it is a manifold of the Schwabe cycle and the Hale cycle. The calculation of the AHR signal shows that the periods vary from 34 to 77 years with an average value of 57.2 years. It is rather surprising that the actual periods vary so much since it is a question of the effects caused by the orbits of Jupiter and Saturn. According to Figure 5, the SSB movements also have a small impact on the 88-year cyclicity amplitude.

The two strong cyclic signals of 60-year (AHR) and 88-year (Gleissberg) periodicity are probably the greatest cosmic driving forces of the surface temperature. The combination of these signals is calculated and depicted in Figure 7. The AHR signal is from the study of Ollila (2017) by standardizing it from –100 to +100%. The amplitude of the 88-year Gleissberg signal has been fitted to give the same maximum and minimum amplitude values as the AHR signal by standardizing the amplitude of a sinusoidal signal of 88-year Gleissberg from –100 to 100 %.

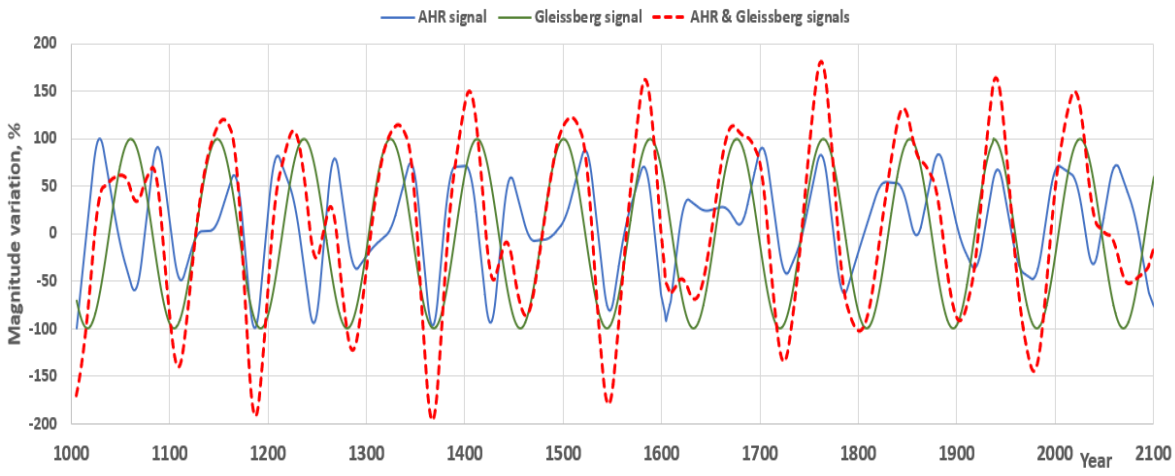

Figure 7. The AHR signal and Gleissberg signal and their combination by assuming similar amplitudes.

The maximum of the AHR signal happened in 1941. Peristykh and Damon (2003) have concluded that the maximum peak of the Gleissberg cycle happened in 1939. In this study, the timing of the Gleissberg cycle has been fitted to give the maximum in 1937, which is the year of the solar cycle maximum, and this choice produces the grand maximum for the combined signal for the year 1940. The end of the 1930s is the well-known temperature maximum period of global temperature trends as can be seen in Figure 1. The depicted trend of the AHR and the Gleissberg cyclic signals has been depicted in Figure 8 together with the FTPC tree-ring curve.

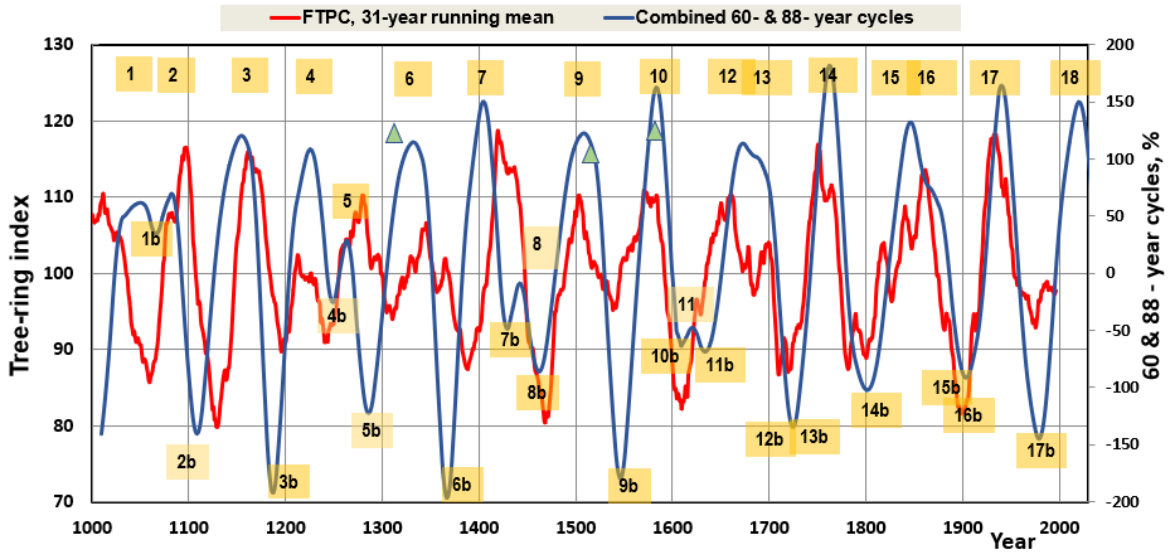

Figure 8. FTPC 31-year running mean signal and combined AHR & Gleissberg signal. The three triangles are the signal values of Crowley & Lowery's 31-year running mean signal.

Near the peaks 4, 6, and 7 are depicted the amplitude peak values of Crowley & Lowery, which show that probably the FTPC data peaks of this time have been dampened by volcanic-type activities. The heavier 31-year smoothing of the FTPC signal covers some details of shorter periodicity but the overall impact of this signal shows excellent correspondence with the AHR & Gleissberg signal variations. The small peak 5 impacts can be found in the FTPC data but peaks 8 and 11 have been smoothed out in the 31-year running average. The grand maximum points of time (AHR and Gleissberg signal happen at the same time) are the years 1406, 1583, 1762, 1940, and 2020, and the grand minimum time points are 1187, 1367, 1546, and 1978, which have also been depicted in Figure 3. These temperature extremes can be found in Figure 3 in all tree-ring proxies and it matches the forcing signal of AHR and Gleissberg cyclicity. It means that the timing of the AHR & Gleissberg signals has been fitted correctly into the yearly time scale.

The cyclicity fitting of the AHR and Gleissberg signals was the primary objective of this study. Even though it was an assumption in combining the AHR and Gleissberg signals such that they have the same maximum and minimum effects, the combined amplitude effects of these two signals seem to fit very well into the FTPC amplitude variations in Figure 7.

It should be noticed that the AHR signal varies from 35 to 77 years and the Gleissberg cyclicity varies from 79 to 91 years. Therefore, the temperature effects do not follow each other in the accurate periods of time but the overall effect is in average 60-years and 88-year periods anyway.

4 Conclusions and Discussion

The main conclusion is that the well-known Gleissberg of about 88-year cycle length is the major periodicity of the data applied. This cyclicity change is related to the Sun's long-term activity changes which can be connected to the repetitive occurrence of the basic solar Schwabe cycle of 11 years (varying from 10 to 14 years) as well to the Hale 22-year cycle. The about 60-year temperature oscillations are observed in global proxy temperature series, and in regional areas key figures like AMO and PMO are real. This occurrence is not related to the Schwabe cycle but it can be connected to the AHR oscillations caused by the Sun's movements around the solar system barycenter (SSB) having the same oscillation pattern, and the analysis shows that the relationship is statistically moderate. This result is rather good since stochastic volcanic eruptions deteriorate the temperature dependency.

This work did not cover the magnitude effects of AHR on the global temperature. An earlier study by Ollila (2017) has shown that a semi-empirical climate model (SECM) including AHR, TSI, greenhouse gas effects, and major volcanic eruptions could simulate the global temperature changes from 1630 to 2015 with a standard error of 0.09 °C and with the coefficient of determination $r^2 = 0.9$.

It can be estimated from the data applied in Figure 2 that the temperature oscillation amplitude in the northern hemisphere varies from 0.31 °C to 0.42 °C, and the same of the global GSMO varies from 0.21 °C to 0.38 °C. The global oscillation amplitude of about 0.30 °C has a significant effect on the global temperature variation and it should be included in the climate model qualities.

The results of this study conflict with the results of Mann et al. (2021) that the apparent multidecadal 50- to 70-year oscillations are an artifact of pulses of volcanic activity. In this study, powerful volcanic eruptions are stochastic disturbances that can cause temperature decreases, but they cannot explain general temperature oscillation patterns of about 60-year AHR cycles and the origin of about 88-year Gleissberg cycles.

Since AHR and the TSI mechanism happen through changes in cloudiness, Ollila (2017) has proposed that the AHR effect depends on the TSI magnitude in a linear way. When TSI is at a maximum level, as in the 2000s, the AHR effect is also at maximum, meaning the climate is sensitive to decreases in cloudiness. When the TSI level is at a minimum level, as during the LIA, the AHR effect is at a minimum, since low TSI magnitude is already causing a high cloud fraction, and the AHR cannot increase it anymore. This proposed mechanism could be related to the Hallstatt cycle of 2100-2500 years, which according to the analysis of Scafetta et al. (2016) has a grand maximum of around 2000 based on residual $\Delta^{14}C$ (‰) analysis during the Holocene. The findings of this study support the conclusion that the 60 & 88 – years cycles have their grand maximum impacts in around 1939 and 2000-2020 but thereafter the impact of these cycles weakens during the rest of the century. Since solar activity has been slightly declining from 2000 onward *according to CERES observations (Ollila, 2021),* it means that warming of the Earth *originating from*

solar and other natural periodicities should not increase during the 2020 decade and decrease gradually thereafter.

There are not enough long-term observations about cosmic dust variations in the atmosphere so far. The dust amounts in ocean sediments and the ice-core samples are so small that reliable trends cannot be observed.

We propose that the AHR effect happens through variations of cosmic dust entering the atmosphere, and these variations cause cloudiness variations that have a strong effect on surface temperature. Cloudiness changes have a significant impact on shortwave (SW) radiation changes and surface temperature. According to CERES satellite measurements, the SW radiation increased by 1.61 Wm^{-2} from 2001 to 2019 (Ollila 2021, Loeb et al., 2021), which can be compared to the CO_2 radiative forcing of 2.16 Wm^{-2} from 1750 to 2019 (IPCC, 2021). According to Loeb et al. (2018), the correlation between SST and low cloud cover is robust**.**

We thank the Natural Resources Institute Finland for the data access for the supra-long Scots pine tree-ring record for northern Finnish Lapland.

Statements

The authors have not received external funding for this research work.
No conflict of interest exists.

References

Agnihotri, R., Dutta. K., Bhushan, R., & Somayajulu B. L.,K. (2002) Evidence for solar forcing on the Indian monsoon during the last millennium. *Earth and Planetary Science Letters,* **198**, 521-527. https://doi.org/10.1016/S0012-821X(02)00530-7

Attolini, M. R., Cecchini, S., Galli, M., & Nanni, T. (1987) *The Gleissberg and 130-year periodicity in the cosmogenic isotopes in the past: The Sun as a quasi-periodic system.* Paper presented in Proceedings of the 20th International Cosmic Ray Conference, Moscow, **4**, 323, Nauka, Moscow.

Bellomo, K., Murhpy, L. N., Cane, M. A., Clement, A. C., & Polvani, L. M. (2018) Historical forcings as main drivers of the Atlantic multidecadal variability in the CESM large ensemble. *Climate Dynamics*, **50**, 3687–3698. https://doi.org/10.1007/s00382-017-3834-3 .

Bellucci, A., Mariotti, A., & Gualdi, S. (2017) The role of forcings in the 20th century North Atlantic multi-decadal variability: the 1940-1975 North Atlantic cooling case study. *Journal of Climate,* **30**, 7317-7337. https://doi.org/10.1175/JCLI-D-16-0301.1 .

Booth, B. B., Dunstone, N. J., Haleoran, P. R., Andrews, T., & Bellouin, N. (2012) Aerosols implicated as a prime driver of 20th century North Atlantic climate variability. *Nature,* **484**, 228-232. https://doi.org/10.1038/nature10946 .

Briffa, K. R., Osborn, T. J., Schweingruber, F. H., Harris, I. C., Jones, P. D., Shiyatov, S. G., & Vaganov, E. A. (2001) Low-frequency temperature variations from a northern tree ring density network. *Journal of Geophysical Research: Atmospheres,* **106**, 2929–2941. https://doi.org/10.1029/2000JD900617 .

Cane, M. A., Clement, A. C., Murhpy, L. N., & Bellomo, K. (2017) Low-pass filtering, heat flux, and Atlantic multidecadal variability. *Journal of Climate,* **30**, 7529-7553. https://doi.org/10.1175/JCLI-D-16-0810.1 .

Carrillo-Sánchez, J. D., Nesvorný, D., Pokorný, P., Janches, D., Plane, J. M. C. (2016) Sources of cosmic dust in the Earth's atmosphere. *Geophysical Research Letters,* **43**(23), 11,979–11,986. doi:10.1002/2016GL071697 .

Chen, D., Wang, H., Sun, J., Gao Y. (2016) A multidecadal oscillation in the northeastern Pacific, *Atmospheric and Oceanic Science Letters*, 9:4, 315-326, DOI: 10.1080/16742834.2016.1194716 .

Cini Castagnoli, G., Bonino, G., Serio, M., Sonett, C. P. (1992) Common spectral features in the 5500-year record of total carbonate in sea sediments and radiocarbon in tree rings. *Radiocarbon*, **34**(3), 798–805. DOI: 10.1080/16742834.2016.1194716

Clement, A., Bellomo, K., Murphy, L. N., Cane, M, A., Mauritsen, T., Radel, G., & Stevens, B. (2015) The Atlantic Multidecadal Oscillation without a role for ocean circulation. *Science,* **350**, 320-324. DOI: 10.1126/science.aab3980 .

Clement, A., Cane, M. A., Murphy, L. N., & Bellomo, K. (2016) Response to comment on "The Atlantic Multidecadal Oscillation without a role for ocean circulation". *Science,* **352**, 1527-1527. DOI: 10.1126/science.aaf2575 .

DelSole, T., Tippett, M. K., & Shukia, J. (2011) A significant component of unforced multidecadal variability in the recent acceleration of global warming. *Journal of Climate,* **24**, 909-926. https://doi.org/10.1175/2010JCLI3659.1 .

Dermott, S. F., Jayaraman, S., Xu Y.-L., Gustafson, Å. S., & Liou, J. C. (1994) A circumsolar ring of asteroidal dust in resonant lock with the Earth. *Nature,* **369**, 719–723. https://doi.org/10.1038/369719a0 .

Dunne, E. M., Gordon, H., Kurten, A., Almeida, J., Duplissy, J., et al. (2016) Global atmospheric particle formation from CERN CLOUD measurements. *Science,* **364**(6316), 1119-1124. doi:10.1126/science.aaf2649 .

Enfield, D. B., Mestas-Nunez, A. M., &Trimble, P. J. (2001) The Atlantic Multidecadal Oscillation and its relation to rainfall and river flows in the continental U.S. *Geophysical Research Letters,* **28**, 2077-2080. https://doi.org/10.1029/2000GL012745 .

Ermakov, V. J., Okhlopkov, V. P, & Stozhkov, Yu. I. (2009) Influence of cosmic rays and cosmic dust on the atmosphere and Earth's climate. *Bulletin Russian Academy Sciences: Physics,* **73**, 434-436. https://doi.org/10.3103/S1062873809030411 .

Feynman, J., & Fougere, P. F. (1984), Eighty-eight year periodicity in solar terrestrial phenomena confirmed *Journal of Geophysical Research: Space Physics,* **89**, 3023–3027. https://doi.org/10.1029/JA089iA05p03023 .

Folland, C. K., Parker, D., E, & Kates, F. E. (1984) Worldwide marine temperature fluctuations 1856–1981. *Nature,* **310**, 670–673. https://doi.org/10.1038/310670a0 .

Folland, C. K., Parker, D. E., & Kates, F. E. (1986) Sahel rainfall and worldwide sea temperatures, 1901-85. *Nature,* **320**, 602-607. https://doi.org/10.1038/320602a0 .

Frankcombe, L. M., England, M. H., Mann, M. E., & Steinmann, B., A. (2015) Separating Internal Variability from the Externally Forced Climate Response. *Journal of Climate,* **29**, 8184-8202. https://doi.org/10.1175/JCLI-D-15-0069.1 .

Gao, C., Robock, A., Self, S., Witter, J. B., Steffenson, J. P., & Clausen, H. B., et al. (2006) The 1452 or 1453 AD Kuwae eruption signal derived from multiple ice core records: Greatest volcanic sulfate event of the past 700 years. *Journal of Geophysical Research,* **111**, D12017. https://doi.org/10.1029/2005JD006710 .

Gardner, C. S., Liu, A. Z., Marsh, D. R., Feng, W., Plane, J. M. C. (2014) Inferring the global cosmic dust influx to the Earth's atmosphere from lidar observations of the vertical flux of mesospheric Na. *Journal of Geophysical Research: Space Physics,* **119**(9), *7870–7879.* doi:10.1002/2014JA020383 .

GISS. *Gistemp temperature set,* (2020) Data is available at https://data.giss.nasa.gov/gistemp/tabledata_v3/GLB.Ts+dSST.txt.

Gleissberg, W. (1958) The eighty-year sunspot cycle, *Journal of British Astronomical Association,* **68**,148–152.

Gold, T. (1975) Resonant orbits of grains and the formation of satellites. *Icarus*, **25**, 489-491. https://doi.org/10.1016/0019-1035(75)90016-0 .
HadCRUT

Haustein, K., Otto, F. E. L., Venema, V., Jacobs, P., Cowtan, K., Hausfather, Z., et al. (2018) A Limited Role for Unforced Internal Variability in Twentieth-Century Warming. *Journal of Climate*, **32**, 4893-4917. https://doi.org/10.1175/JCLI-D-18-0555.1 .

Hale, G. E. (1908) On the Probable Existence of a Magnetic Field in Sun-Spots. *Astrophysical Journal*, **28**, 315-343.

Helama, S., Lindholm, M., Timonen, M., Eronen, M., & Meriläinen, J. (2002) Part 2: Interannual-to-centennial variability in summer temperatures in northern Fennoscandia during the last 7500 years extracted from tree-rings of Scots pine. *The Holocene*, **12**, 681-687. https://doi.org/10.1191/0959683602hl581rp .

Humlum, O., Stordal, K., & Solheim, J.-E. (2013) The phase relation between atmospheric carbon and global temperature. *Global and Planetary Change*, **100**, 51-69. https://doi.org/10.1016/j.gloplacha.2012.08.008 .

IPCC, AR6, Climate Change (2021) *The Physical Science Basis. Contribution of Working Group I to the Sixth Assessment Report of the Intergovernmental Panel on Climate Change,* Cambridge University Press, Cambridge, United Kingdom and New York, NY, USA, 2391 pp.

Kalliokoski, M., Gudmundsdottir, E.R., Westergård, S. (2020). Hekla 1947, 1845, 1510 and 1158 tephra in Finland: challenges of tracing tephra from moderate eruptions. *Journal of Quaternary Science*, 35(6), 803–816.

Kerr, R. A. (2000) A North Atlantic Climate Pacemaker for the Centuries. *Science*, **288**,1984-1985. DOI: 10.1126/science.288.5473.1984 .

Klyashtorin, L. B., Borisov, V., & Lyubushin, A. (2009) Cyclic changes of climate and major commercial stocks of the Barents Sea. *Marine Biology Research*, **5**, 4-17. https://doi.org/10.1080/17451000802512283 .

Knight, J. R. (2009) The Atlantic multidecadal oscillation inferred from the forced climate response in coupled general circulation models. *Journal of Climate*, **22**, 1610-1625. https://doi.org/10.1175/2008JCLI2628.1 .

Krishna, K.C., Durbha, N.H. (2013) Cosmic dust – a Problem? Or a solution? *6th International Conference on Recent Developments in Space Technologies (RAST).* 12-14 June 20913, Istanbul, Turkey.

Lean. J, Beer, J., & Bradley, R. (1995) Reconstruction of solar irradiance since 1610: Implication for climate. *Geophysical Research Letters*, **22**, 3195-3198. DOI: 10.1029/95GL03093 .

Lin, Y. C., Fan, C. Y., Damon, P. E., & Wallick, E. I. (1975) *Long-term modulation of cosmic-ray intensity and solar activity cycles*, Paper presented in 14th International Cosmic Ray Conference, Germany, Munchen, 3:995–999. Max-Planck-Institut für extraterrestrische Physik, Germany.

Ljungqvist, F. C. (2010) A new reconstruction of temperature variability in the extra-tropical Northern Hemisphere during the last two millennia. *Geografiska Annaler, Series A: Physical Geography,* **92 A**, 339-351. https://doi.org/10.1111/j.1468-0459.2010.00399.x. Data available at https://www1.ncdc.noaa.gov/pub/data/paleo/contributions_by_author/ljungqvist2010/ .

Loeb, N. G., Thorsen, T. J., Norris, J. R., Wang, Su W. (2018) Changes in earth's energy budget during and after the "pause" in global warming: An observational perspective. *Climate*, **6**, 62. https://www.mdpi.com/2225-1154/6/3/62 .

Loeb, N. G., Johnson, G. C., Thorsen, T. J., Lyman, J. M., Rose, F. G., Kato, S. (2021) Satellite and Ocean Data Reveal Marked Increase in Earth's Heating Rate. *Geophysical Research Letters,* 48, e2021GL093047. https://doi.org/10.1029/2021GL093047 .

FTPC, *The supra-long Scots pine tree-ring record for Finnish Lapland,* (2020) Available at http://lustialab.com/data/Advance/adv7638.exz .

Lüdecke, H.-J., Cina, R., Dammschneider, H.-J., & Lüning, S. (2020) Decadal and multidecadal natural variability in European temperature. *Journal of Atmospheric and Solar-Terrestrial Physics,* **205**, 105294. https://doi.org/10.1016/j.jastp.2020.105294 .

Mann, M. E., Steinman, B. A., & Miller, S. K. (2014) On forced temperature changes, internal variability, and the AMO. *Geophysical Research Letters,* **41**, 3211-3219. https://doi.org/10.1002/2014GL059233 .

Mann, M. E., Steinman, B. A., Brouillette, D. J., & Miller, S. K. (2021) Multidecadal climate oscillations during the past millennium driven by volcanic forcing. *Science,* **371**, 1014-1019. DOI: 10.1126/science.abc5810 .

NASA, Jet Propulsion Laboratory, *Horizon Web-interface*, (2022) Application is available at http://ssd.jpl.nasa.gov/horizons.cgi .

Metoffice Hadley Centre, *HadCRUT4 temperature data set,* (2022) Data is available at https://www.metoffice.gov.uk/hadobs/hadcrut4/data/current/time_series/HadCRUT.4.6.0.0.annual_ns_avg.txt .

Mikkonen, S., Laine, M., Mäkelä, H. M., Gregow, H., Tuomenvirta, H., Lahtinen, M. et al. (2015) Trends in the average temperature in Finland, 1847–2013. *Stochastic Environmental Research and Risk Assessment,* **29,** 1521-1529. https://doi.org/10.1007/s00477-014-0992-2

Murhpy, L. N., Bellomo, K., Cane, M., & Clement, A. (2017) The role of historical forcings in simulating the observed Atlantic multidecadal oscillation. *Geophysical Research Letters,* **44**, 2472-2480. https://doi.org/10.1002/2016GL071337 .

NAS, National Academy of Sciences (1975). *Understanding climate change, a program for action.* Washington D.C., p 239. United States Committee for the Global Atmospheric Research Program.

Nesvorný, D. Jenniskens, P., Levison, H., Bottke, W. F, Vokrouhlický, D., Gounelle, M. (2010) Cometary origin of the zodiacal cloud and carbonaceous micrometeorites. Implications for hot debris disks. *The Astrophysical Journal,* **713**(2), 816–836. doi:10.1088/0004-637X/713/2/816 .

NOAA, *National temperature time series of USA*, (2022a) Data is available at https://www.ncei.noaa.gov/access/monitoring/climate-at-a-glance/national/time-series .

NOAA. *Atlantic Multidecadal Oscillation AMO, (*2022b) Data is available at https://psl.noaa.gov/data/correlation/amon.us.long.data .

NSDC, *Six tree-ring proxy data and one temperature data set*, (2020) Data is available at https://www1.ncdc.noaa.gov/pub/data/paleo/treering/reconstructions/n_hem_temp/briffa2001jgr3.txt .

Ollila, A. (2016) Climate sensitivity parameter in the test of Mount Pinatubo eruption. . *Physical Science International Journal,* **9**(4), 1-14. DOI: 10.9734/PSIJ/2016/23242 .

Ollila, A. (2017) Semi empirical model of global warming including cosmic forces, greenhouse gases, and volcanic eruptions. *Physical Science International Journal,* **15**(2), 1-14. DOI: 10.9734/PSIJ/2017/34187 .

Ollila, A. (2021) Global circulation models (GCMs) simulate the current temperature only if the shortwave radiation anomaly of 2000s has been omitted. *Current Journal of Applied Science and Technology,* **40**(17), 42-52.

Ogurtsov, M. G., Nagovitsyn, Yu. A., Kocharov, G. E., & Jungner, H. (2002) Long-Period Cycles of the Sun's Activity Recorded in Direct Solar Data and Proxies. *Solar Physics,* **211**, 371–394. https://doi.org/10.1023/A:1022411209257 .

Ogurtsov, M. G., Raspopov, O. M. (2011) Possible impact of interplanetary and interstellar dust fluxes on the Earth's climate. *Geomagnetism and Aeronomy*, **51**(2), 275–283. doi:10.1134/s0016793211020137 .

Patterson, R. T., Prokoph, A., Changa, A. (2004) Late Holocene sedimentary response to solar and cosmic ray activity influenced climate variability in the NE Pacific. *Sedimentary Geology*, **172** , 67 – 84. https://doi.org/10.1016/j.sedgeo.2004.07.007 .

Peristykh, A. N., & Damon, P. E. (2003) Persistence of the Gleissberg 88- year solar cycle over the last ~ 12,000 years: Evidence from cosmogenic isotopes. *Journal of Geophysical Research: Space Physics*, **108** (A1), 1003. https://doi.org/10.1029/2002JA009390 .

Plane, J. M. C. (2012) Cosmic dust in the earth's atmosphere. *Chemical Society Reviews*, **41**(19), 6507–6518. doi:10.1039/c2cs35132c .

Rayner, N. A., Parker, D. E., Horton, E. B., Folland, C. K., Alexander, L. V., Rowell, D. P. et al. (2003) Global analyses of sea surface temperature, sea ice, and night marine air temperature since the late nineteenth century. *Journal of Geophysical Research: Atmospheres*, **108,** 4407. https://doi.org/10.1029/2002JD002670 .

Roberts, P. H., Yu, Z. J., & Russell, C. T. (2007) On the 60-year signal from the core. *Geophysical & Astrophysical Fluid Dynamics*, **101**, 11-35. https://doi.org/10.1080/03091920601083820 .

Rohde, R., Muller, R. A., Jacobsen, R., Muller, E., Perlmutter, S., Rosenfeld, A. et al. (2013) A New Estimate of the Average Earth Surface Land Temperature Spanning 1753 to 2011. *Geoinformatics & Geostatistics: An Overview*, **1**(1), 1-7. doi:10.4172/2327-4581.1000101.

Rojas, J., Duprat, C., Engrand, C., Dartois, E., Delauche L., Godard, M., Gounelle, M., Carillo-Sanchez, J. D., Pokorny, P., Plane, J. M. C. (2021) The micrometeorite flux at Dome C (Antarctica), monitoring the accretion of extraterrestrial dust on Earth. *Earth and Planetary Science Letters*, **560**, 116794. https://doi.org/10.1016/j.epsl.2021.116794

Scafetta, N. (2010) Empirical evidence for a celestial origin of the climate oscillations and its implications. *Journal of Atmospheric and Solar-Terrestrial Physics*, **72**(13), 951–970. https://doi.org/10.1016/j.jastp.2010.04.015 .

Scafetta, N., Milani, F., Bianchini, A., & Ortolani, S. (2016) On the astronomical origin of the Halestatt oscillation found in radiocarbon and climate records throughout the Holocene. *Earth-Science Reviews*, **162**, 24-43. https://doi.org/10.1016/j.earscirev.2016.09.004 .

Svensmark, H. (1998) Influence of cosmic rays on earth's climate. *Physical Review Letters,* **81**, 5027-5030. https://doi.org/10.1103/PhysRevLett.81.5027 .

Schlesinger, M. E. & Ramankutty, N. (1994) An oscillation in the global climate system of period 65-70 years. *Nature*, **367**, 723-726. https://doi.org/10.1038/367723a0 .

Schwabe, S. H. (1843) Sonnenbeobachtungen im Jahre 1843 (in German). Observations of the Sun in the year 1843. *Astronomische Nachrichten,* **21**, 233–236.

Siscoe, G. L. (1980) Evidence in the auroral record for secular solar variability. *Reviews of Geophysics,* **18**, 647–658. https://doi.org/10.1029/RG018i003p00647 .

Suess, H. E. (1980) The radiocarbon record in tree rings of the last 8000 years. *Radiocarbon,* **22**(2), 200– 209. https://doi.org/10.1017/S0033822200009462 .

Trenberth, K. E. & Shea, D. J. (2006) Atlantic hurricanes and natural variability in 2005. *Geophysical Research Letters,* **13**, L12704. https://doi.org/10.1029/2006GL026894 .

Ting, M., Kushnir, Y., Seager, R., & Li, C. (2009) Forced and internal twentieth-century SST trends in the North Atlantic. *Journal of Climate,* **22**, 1469-1481. https://doi.org/10.1175/2008JCLI2561.1 .

Wu, S., Liu, Z., & Zhang, R. (2011) On the observed relationship between the Pacific Decadal Oscillation and the Atlantic Multi-decadal Oscillation. *Journal of Oceanography,* **67**, 27-3. https://doi.org/10.1007/s10872-011-0003-x .

Wyatt, M. C., Dermott, S. F., & Grogan, K. (1999) *A unique view through the Earth's resonant ring.* Astrophysics with infrared surveys: A prelude to SIRTF, ASP Conference Series, 177, p. 374-380.

Zanchettin, D., Bothe, O., Muller, W., Bader, J., & Jungclaus, J. H. (2014) Different flavors of the Atlantic Multidecadal Variability. *Climate Dynamics,* **42**, 381-399. https://doi.org/10.1007/s00382-013-1669-0 .

Zhang, R. (2017) On the persistence and coherence of subpolar sea surface temperature and salinity anomalies associated with the Atlantic multidecadal variability. *Geophysical Research Letters,* **44**, 7865-7875. https://doi.org/10.1002/2017GL074342 .

Appendix

Replies to concerns

Reference. Ollila, A., Timonen, M. (2022). Two main temperature periodicities related to planetary and solar activity oscillations. International Journal of Climatology, 1-15.

We have analyzed each concern and individually replied to each concern.

1. Section 1 – Introduction, second paragraph - It is stated that "The IPCC has never included the AMO effects in its GCM (general climate model) temperature simulations." However, no reference is provided regarding this claim. This cannot be deduced from the summary report.

   Reply. The statement that "the IPCC has never included the AMO effects in its GCM simulations" should be reformulated to cover only the CMIP5 (Coupled Model Intercomparison Project - Phase 5) models since we have no evidence about the earlier generation models: "the IPCC has never included the AMO effects in its GCM simulations per CMIP5". Michel Mann (2014) has concluded from CMIP5 control runs covering the last millennium that the GCMs could reveal only ENSO-type periodicities but no AMO-like 40-60-year periods. Of course, it is also a question if models have been constructed to include observational evidence of 60–80-year oscillations or it is a question that the GCMs could not identify any evidence about these periods in the proxy data applied in simulation runs. Even though tree ring data is year-accurate, it is also sensitive for averaging procedures which may easily destroy periodicities.

   The summary of Effective Radiative Forcings from 1750 to 2019 in Fig. 7-6 does not include any natural forcings except solar forcing.

2. Section 2.1, last sentence – It is stated that "…the PMO index from Chen et al. (2016)", reference not included in the reference list. Instead, one may find the following: Chen, D., Wang, H., Sun, J., & Gao, Ya. (2018) Pacific multi-decadal oscillation modulates the effect of Arctic oscillation and El Niño southern oscillation on the East Asian winter monsoon. International Journal of Climate, 38, 2808-2818. https://doi.org/10.1002/joc.5461. However, the above doi, authors, and title, point to an article of the International Journal of Climatology and not of the International Journal of Climate. Is this reference instead meant to read: "Dong CHEN, Hui-Jun WANG, Song YANG & Ya GAO (2016) A multidecadal oscillation in the northeastern Pacific, Atmospheric and Oceanic Science Letters, 9:4, 315-326, DOI: 10.1080/16742834.2016.1194716"?

Reply. As noticed in the concern, the article in the reference list has been partly wrongly typed, and it should be "Chen, D., Wang, H., Sun, J., Gao Y. (2016) A multidecadal oscillation in the northeastern Pacific, Atmospheric and Oceanic Science Letters, 9:4, 315-326, DOI: 10.1080/16742834.2016.1194716".

3. Section 2.1, the PMO is provided only in form of a graph and not as a time series of values that could be used for further analysis. The source of this data is not provided.

   Reply. The authors have digitized the original graph of Chen et. al (2016) as explained in the caption of Fig. 3 since the digital values of the original graph were not available to the authors. We think that it is not appropriate to include these digitized values in our paper since their accuracies are not the same as the original values. On the other hand, these digitized values have been used only for creating a graphical curve, and the actual values have been not applied in any mathematical analyses of this study. The graphical curves in Fig. 3 have been used to illustrate the characteristics of the four different signals so that a reader can estimate by eye the similarities of these signals.

4. Section 2.2, last sentence – It is stated that "…applying a second-order differential equation $T = 517.29 - 0.2587 * yr + 0.00006805 * yr^2$."

   Reply. This equation has been wrongly named to be differential but it is a second-order polynomial equation.

5. Despite the fact that the above formula corresponds to a second order polynomial and not to a differential equation, no explanations are provided:
   a. On why this specific detrending method has been selected?
   b. Why this is the optimal polynomial degree?
   c. What may be the eventual impact of this detrending on the results produced by the detrended time series?

   Reply. It should be noticed that the choice of detrending methods is unlimited just thinking for example possible polynomial fittings. In this case, the detrending method was selected considering the relatively long periodicities (from 60 to 90 years) of the temperature, its nonlinearly growing value from 1880 onward, and the strong yearly variations. It was quickly noticed that a nonlinear fitting equation is needed. A polynomial equation was selected based on the options of Excel, and it is shown in the Methods. This selection is illustrated in Figure 1.

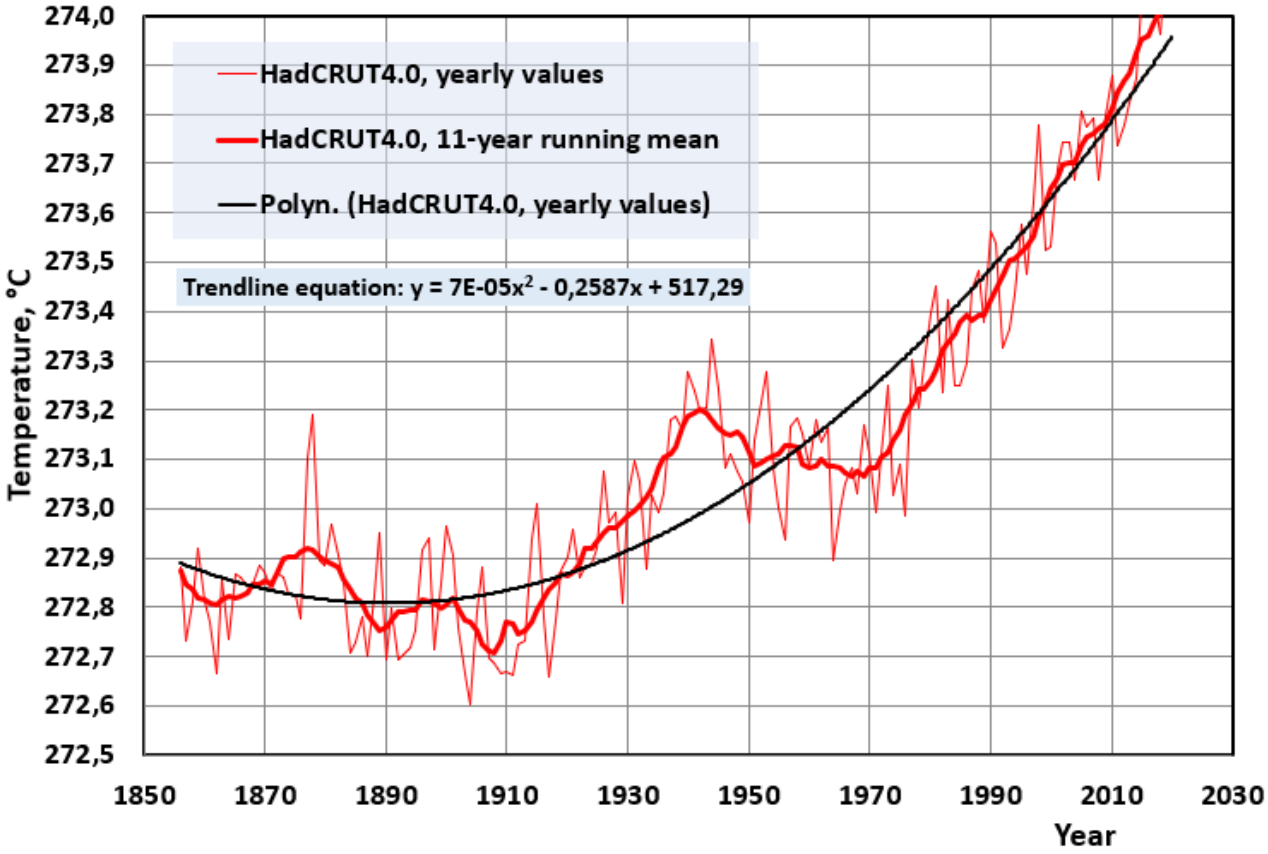

Figure 1. Yearly, 11-year running mean, and trendline selection were used for detrending HadCRUT4.0 temperature data.

The impact of the selected detrending method can be assessed to be insignificant. The purpose of the detrending method in this case is to elicit the possible long-term variations of the global temperature. Without an appropriate detrending method the periodicity of about 60 years would be very difficult to notice. Thinking of the result, the selected detrending method can be estimated to be good enough. The detrended data of temperature (HadCRUT4.0) has not been used for any statistical or digital analyses. Therefore, the authors have used only moderate efforts to select a detrending method.

6. Section 3.1, first sentence – Reference is made to Ermakov et al. (2019). However, this reference is flawed since in the abstract one reads "A forecast of the climate cooling in the forthcoming 50 years is given.", a claim which observational data until this date have proven that it is false.

Reply. This first reference to Ermakov et al. (2009) was giving credit to them for introducing first the idea that planetary orbits have an influence mechanism on temperature variations. The forecast of Ermakov et al. (2009) can be criticized in that

they have not considered other climate forcing factors than the planetary effects, and therefore their forecast till today is not looking strong.

7. Section 3.1, last paragraph – It is stated that "Ermakov et al. (2009) have proposed that the varying amounts of dust entering the atmosphere change the cloudiness and, further, cause temperature variations." However, this statement is contradicted by Dunne et al. (2016), a reference that the authors have used a few lines before. In the abstract of this reference it is stated: "A considerable fraction of nucleation involves ions, but the relatively weak dependence on ion concentrations indicates that for the processes studied, variations in cosmic ray intensity do not appreciably affect climate through nucleation in the present-day atmosphere."

   Reply. The nucleation process dependence on cosmic ray intensity was first introduced by Svensmark and Friis-Christensen (1997). This theory was questioned for example by Kernthaler et al (1999). Svensmark et al. (2009) found later a good correlation between low-level clouds better than total cloudiness. This theory has remained under debate all these years. Interestingly enough, this theory has come forth recently in connection to shortwave anomalies observed by CERES satellites. Loeb et al. (2018) have found that the decreases in low cloud cover were primary drivers of the decreases in reflected SW fluxes at the TOA and this correlation is robust. The question remains: What causes changes in low-level clouds? Reasonable proposals are cosmic ray fluxes and cosmic dust amounts entering the atmosphere.

8. Section 3.2, Figure 2 – No reference demonstrating that the data presented in Figure 2 have been peer reviewed is provided.

   Reply. The data in Figure 2 is hypothetical, just showing the principle of how cross-dating works. This kind of basic technics of dendrochronology has not been explained or referred to in the publications of dendrochronoly.

9. Section 3.2 – It is stated that "but the temperature estimates obtained from the modeling are easy to scale to correspond to the variation in the temperature-measurement data." However, no reference is provided, and it is not explained how this scaling can be performed.

   Reply. In this research paper tree-ring data has not been converted into temperatures and this issue is not in the scope of this study. The details of converting tree ring widths to temperatures are explained in the main paper of the FTPC analyses (Helama et al., 2002).

10. Section 3.4, page 10415 – It is stated that "There is a logical explanation as to why the volcanic eruptions in Iceland have a strong influence on the temperatures and tree growth in Finland. The reason is the westerly wind pattern, which is dominant in Finland, and these winds in the troposphere bring a lot of volcanic ash particles to

Scandinavia from Iceland." However, no reference is provided, and no wind climatology data are presented to support this claim.

Reply. The Finnish Meteorological Institute (https://en.ilmatieteenlaitos.fi/climate-elements) states that "*Since Finland is located in the zone of westerly air disturbances, there are great variations in air pressure and winds, especially in winter. In the whole country, the wind blows most commonly from the southwest and least commonly from the northeast." See also the next concern.*

11. Section 3.4, page 10415 - It is stated that "Therefore, the impacts of lower severity index eruptions like VEI 3 in Iceland may have the same impact as VEI 6–7 index in other parts of the world." However, no reference is provided, and also no proof for this hypothesis.

    Reply. It has been well-known that the Islandic volcanic eruptions spread ash to Scandinavian countries. Kalliokoski et al. (2020) have carried out a survey study of these effects and they summarize the findings in this way: "*Our results confirm that Icelandic eruptions of moderate size can form cryptotephra deposits that are extensive enough to be used in inter-regional correlations of environmental archives and carry a great potential for refining regional tephrochronological frameworks. Our results also reveal that Icelandic tephra has been dispersed into Finnish airspace at least seven times during the past millennium and in addition to a direct eastward route the ash clouds can travel either via a northerly or a southerly transport pathway*."

12. Section 4, page 10418 – It is stated that "…the TSI mechanism happen through changes in cloudiness." The authors do not clarify what do they mean by "the TSI mechanism".

    Reply. TSI mechanism means the same mechanism which has caused changes in SW radiation since 2001 and which is caused by low-level cloud changes.

13. Section 4, page 10418 – It is stated that "Since the solar activity has been slightly declining from 2000 onward, it means that warming of the Earth should not increase during the 2020 decade and decrease gradually thereafter." This claim is not supported by any scientific evidence.

    Reply. The results of this study show that the 60-90-year periods have had maximums from 2000 to 2020, which means that their effect on temperature will decrease during the next 30-45 years.
    We like to add more research results, which have not been referred to in the original paper. The analyses of three Antarctica drill hole samples (Davis et al., 2019) have revealed dominant temperature periods of 724, 745, and 886 years. The temperature

and CO_2 variations are smaller in Antarctica than in Greenland, and therefore same oscillations should be easily found also on the Northern Hemisphere. Dansgaard et al. (1984) and Dansgaard et al., (1993) concluded from the ice-core records of Greenland for the period of 250 000 years that climate has been unstable during glaciation periods, and these climate periods were named Dansgaard – Oeschger oscillations. The periodicities of Greenland's ice-core records according to Vinther et al. (2010) have been 1270, 1470, and 2550 years. In the later article of Vinther (2011), a dominant period is about 1000 years peaking at 1000 and 2000 years.

The mechanism of these very long periodicities are still uncertain but they are real. Davis et al. (2019) have named external forces of the Earth like periodic variations in solar insolation and natural perturbations of Earth's orbital cycles to be probable reasons for variations. Also, Bond (1997) thinks that sea sediment periods found in the North Atlantic area are caused by solar insolation changes. The temperature changes may be relatively quick like the temperature increase after the Little Ice Age in the 1700s or they are slow like the long maximum temperature peak of the Medieval Warm Period from 950 to 1250.

The sun researchers like Zharkova et al. (2015) have developed a double dynamo concept, which simulates very well the Sun’s behavior during the last centuries. This model predicts that the Sun’s activity will decrease during the next 20 years.

14. Section 4, page 10418 – It is stated that "We propose that the AHR effect happens through variations of cosmic dust entering the atmosphere, and these variations cause cloudiness variations". This claim is not supported by any scientific evidence.

Reply. It is a common practice that researchers propose a mechanism for climate drivers, which shows good correlations to temperature variations. For example, this applies to most periodicity research studies, which have been referred to in the Introduction section.

References

Bond, G. (1997) A Pervasive Millennial-Scale Cycle in North Atlantic Holocene and Glacial Climates. *Science*, 278(5341), 1257–1266.

Dansgaard, W., Johnsen, S.J., Clausen, H.B., Dahl-Jensen, D., Gundestrup, N., Hammer, C.U., Oeschger, H. (1984) North Atlantic climatic oscillations revealed by deep Greenland ice cores. *Geophysical Monograph Series Climate Processes and Climate Sensitivity* 29, 288–298.

Dansgaard, W., Johnsen, S.J., Clausen, H.B., Dahl-Jensen, D., Gundestrup, N.S., Hammer, C.U., Hvidberg, C.S., Steffensen, J.P., Sveinbjörnsdottir, A.E., Jouzel, J. (1993). Evidence for general instability of past climate from a 250-kyr ice-core record. *Nature*, 364(6434), 218–220.

Davis, W.J., Taylor, P.J., Davis, W.B. (2019) The origin and propagation of the Antarctic centennial oscillation. *Climate*, 7(9), 11.

Helama, S., Lindholm, M., Timonen, M., Eronen, M., Meriläinen, J. (2002). Part 2: Interannual-to-centennial variability in summer temperatures in northern Fennoscandia during the last 7500 years extracted from tree rings of Scots pine. *The Holocene* 12(6): 681-687.

Kalliokoski, M., Gudmundsdottir, E.R., Westergård, S. (2020). Hekla 1947, 1845, 1510 and 1158 tephra in Finland: challenges of tracing tephra from moderate eruptions. *Journal of Quaternary Science*, 35(6), 803–816.

Kernthaler, C., Toumiand, R. and Haigh, J.D. (1999) Some doubts concerning a link between cosmic ray fluxes and global cloudiness. *Geophysical Research Letters*, 26, 863-865.

Svensmark, H. (1997) Influence of cosmic rays on Earth's climate. *Physical Review Letters* 81, 5027-5030.

Svensmark, H., Bondoand, T. and Svensmark, H. (2009). Cosmic ray decreases affect atmospheric aerosols and clouds. *Geophysical Research Letters*, 36, L15101.

Loeb, N.G., Thorsen, T.J., Norris, J.R, Wang, H. and Su W. (2018). Changes in Earth's energy budget during and after the 'pause' in global warming: An observational perspective. *Climate*, 6(3), 62.

Vinther, B.M., Jones, P.D., Briffa, K.R., Clausen, H.B., Andersen, K.K., Dahl-Jensen, D., Johnsen, S.J. (2010). Climatic signals in multiple highly resolved stable isotope records from Greenland. *Quaternary Science Reviews*, 29(3-4), 522–538.